



## Comparison of numerical schemes for improved prediction model of fecal indicator bacteria in a riverine system

Moonhee Choi<sup>a</sup>, Yongeun Park<sup>a</sup>, Minji Cha<sup>a</sup>, Kyung Hwa Cho<sup>b</sup>, Joon Ha Kim<sup>a,c,\*</sup>

<sup>a</sup>School of Environmental Science and Engineering, Gwangju Institute of Science and Technology (GIST), Gwangju, 500-712, Korea

<sup>b</sup>School of Natural Resources and Environment, University of Michigan, Ann Arbor, MI, 48109, USA

<sup>c</sup>Sustainable Water Resource Technology Center, Gwangju Institute of Science and Technology (GIST), 261 Cheomdan-gwagiro, Buk-gu, Gwangju 500-712, Korea

Tel. +82 62 970 3277; Fax: +82 62 970 2434; email: joonkim@gist.ac.kr

Received 14 October 2011; Accepted 24 December 2011

### ABSTRACT

Different numerical schemes for the fate and transport models of fecal indicator bacteria (FIB) were used to predict the concentration of FIB in a creek, which were then compared to a steady state model (QUAL2E). *Escherichia coli* (EC) and enterococci bacteria (ENT) were selected as representative FIB to compare the model performance under different flow and weather conditions in the Gwangju Creek in Korea. The results revealed that model accuracy of the forward time centered space (FTCS) scheme is the highest compared to the upstream, Dufort-Frankel, Crank-Nicolson methods and steady state model (QUAL2E) under dry weather conditions. In wet weather conditions, however, the upstream scheme shows the best performance among the five models. The upstream scheme thus represented a potential method for predicting the fate and transport of FIB originating from nonpoint sources during the rainy season. This study demonstrates that prediction results could vary in response to different numerical schemes and that the amount of discrepancy between the observed and predicted results can be quite significant. We expect that this study could be applied to the water quality forecasting system as a real time management in near future.

*Keywords:* Fate and transport model; Advection dispersion reaction; Numerical schemes; Fecal indicator bacteria; Nonpoint sources; Meteorological conditions

### 1. Introduction

Water quality deterioration associated with fecal contamination sources is a great concern to human health. However, it should be noted that the presence of fecal bacteria in a water body does not directly imply pathogenic bacteria and that it can indeed be a reasonable indicator of pathogenic organisms derived from a diverse range of human and animal sources. Pathogen-contaminated

recreational water can cause infectious water-related diseases such as gastrointestinal, respiratory, eye, ear, nose, throat, and skin illnesses [1]. As an urban stream in Korea, the Gwangju Creek has been exposed to various fecal contaminations, showing significantly high concentrations of fecal indicator bacteria (FIB; e.g., *Escherichia coli* (EC) and enterococci bacteria (ENT)) [2,3].

To protect public health and freshwater resources, FIB characteristics need to be investigated via intense monitoring and analyses of their fate and transport. For this task, modeling approaches can provide an alternative

\*Corresponding author.

way to efficiently understand the bacteria concentration in a water system [4]. Previous studies have considered the sources, fate, and transport of FIB in a water body and have demonstrated that nonpoint sources (e.g., soil leaching, surface runoff, manure runoff) affect FIB levels as major sources of fecal pollution and that FIB are mainly influenced by weather conditions [5–8]. In particular, the fate of FIB are significantly affected by solar intensity processes under dry weather conditions [9–12] and resuspension processes from the sediment bed under wet weather conditions [13,14]. Eleria and Vogel [15] then found that fecal coliform levels are related to antecedent rainfall, in addition to other hydrological and meteorological variables in the river. For the total maximum daily load (TMDL) development, a modeling approach was suggested as a means for calculating the pollutant load of FIB in the watershed [16], and the fate and transport of pathogens were simulated using hydrodynamic and water quality modules [17–19].

The theoretical basis for the FIB modeling process was proposed by Matson et al. [20], and has since been advanced by several researchers [21–24]. However, numerical schemes for modeling FIB behavior have not been significantly considered. As such, it is thought that different schemes could result in discrepancies among modeling results due to different inherent assumptions and lack of numerical stability [25,26]. Numerical solutions for FIB models can also be affected by the complexity of water flow and weather conditions [27]. Thus, it can be quite challenging to determine a superior numerical scheme for hydrodynamic and water quality modules, especially in view of the complicated conditions noted above. In this study, four different numerical schemes and one steady state model were applied in order to determine the best approach for predicting bacteria concentration in a creek in South Korea. The four different schemes include the upstream, forward time central space (FTCS), Dufort-Frankel, and Crank-Nicolson methods [28,29], and the one steady state model is QUAL2E [30]. These methods are then compared in terms of their accuracy.

Accordingly, the objectives of this study are: 1) to compare model accuracy between the different schemes in terms of ability to predict the concentration of FIB in a creek, and 2) to determine the appropriate method for calculating FIB processes, depending on the underlying weather conditions.

## 2. Materials and methods

### 2.1. Study area

Fig. 1 presents a map of the Yeongsan River and Gwangju Creek (GJC), showing the monitoring stations; black squares (S1, S2, S3, and S4) are FIB monitoring

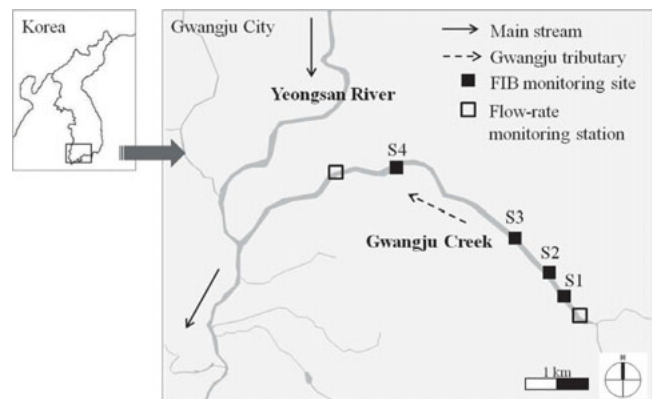


Fig. 1. Gwangju Creek showing the locations of FCB monitoring sites and flow-rate monitoring stations in the region of Gwangju, South Korea.

stations and open squares are flow rate monitoring stations. The GJC is 23.5 km long with a 111.68 km<sup>2</sup> watershed, and it flows through Gwangju Metropolitan City, a highly urbanized area, from Mudeung Mtn. (origin of GJC) to the Yeongsan River [31]. The land use around GJC is characterized as forest area (46.7%) and urban residential and industrial areas (44.3%); it is under the control of the Ministry of Environment, Republic of Korea. On average, there are 129 rainy days and the daily flow rate is ~0.7 m<sup>3</sup>/s. As part of the daily flow rate, 0.5 m<sup>3</sup>/s is an induced environmental flow used to enhance the water quality and to maintain the streamflow, supplied by diverting water from the Yeongsan River into the uppermost stream of the GJC [32].

### 2.2. FIB transport model development

A one-dimensional FIB transport model was developed using a hydrodynamic module in order to predict FIB concentration under dry and wet weather conditions. Here, a FIB sediment storage module was used to simulate the sediment bacteria concentration.

#### 2.2.1. Hydrodynamic model: Saint-Venant equations

For the hydrodynamic model, the Saint-Venant equation was implemented to calculate the water quantity associated with water velocity, water surface elevation, and cross-sectional area. These equations consider the continuity and momentum equations used to reflect local acceleration, convective acceleration, pressure force, gravity force, and friction force [33]:

$$\frac{\partial Q}{\partial x} + \frac{\partial A}{\partial t} = 0 \quad (1)$$

$$\frac{1}{A} \frac{\partial Q}{\partial t} + \frac{1}{A} \frac{\partial}{\partial x} \left( \frac{Q^2}{A} \right) + g \frac{\partial y}{\partial x} - g(S_0 - S_f) = 0 \quad (2)$$

$$S_f = \frac{n^2 Q^2}{A^2 r^{4/3}} \quad (3)$$

where  $t$  is time,  $x$  is distance [m],  $A$  is the cross-sectional area [m<sup>2</sup>],  $Q$  is the discharge [m<sup>3</sup>/s],  $S_f$  is the friction slope [–],  $S_0$  is the bed slope [–],  $r$  is hydraulic radius [m], and  $n$  is the Manning’s coefficient.

2.2.2. FIB transport model: advection dispersion with reaction equation

To simulate the FIB module, the advection dispersion with reaction (ADR) equation was applied by reflecting the flow characteristics, dispersion process, die-off, and resuspension:

$$\frac{\partial C}{\partial t} + u \frac{\partial C}{\partial x} - D \frac{\partial^2 C}{\partial x^2} + kC - R \frac{C_s}{h} = \text{source term} \quad (4)$$

where  $C$  is the FCB concentration [MPN/100 ml],  $u$  is the depth average flow velocity [m/s],  $D$  is the dispersion coefficient [m<sup>2</sup>/s],  $k$  is the first-order decay coefficient [1/s], and  $R$  is the resuspension rate [kg/m<sup>2</sup>s]. In addition,  $C_s$  is the FIB concentration in the sediment bed [MPN/100 g] and  $h$  is the water depth [m].

For the first-order decay coefficient ( $k$ ), the total bacterial die-off rate is a combination of the sunlight die-off rate and the settling rate:

$$k = k_s + f \frac{v_s}{h} \quad (5)$$

$$k_s = \alpha I \quad (6)$$

where  $I$  is the solar intensity with respect to time [MJ/m<sup>2</sup>],  $f$  is the fraction of FIB in the suspended sediment [–],  $v_s$  is the settling velocity of the suspended sediment [m/s], and  $\alpha$  is the FIB die-off constant.

Resuspension from the sediment bed to the water column was reflected as a potential source of FIB:

$$\tau = 3 \times 10^{-3} u^2 \quad (7)$$

where  $\tau$  is the shear stress [N/m<sup>2</sup>]. If the bottom shear stress ( $\tau$ ) is less than the critical shear stress ( $\tau_c$ ), deposition becomes the dominant process. Here, a  $\tau_c$  of 0.75 N/m<sup>2</sup> was determined as the beginning of resuspension.

In addition,  $R$  is the net resuspension process from the sediment bed:

$$R = C_e(\tau/\tau_c - 1) \quad (8)$$

where  $R$  is the resuspension rate [kg/m<sup>2</sup> s] and  $C_e$  is the entrainment coefficient [kg/m<sup>2</sup> s].

2.2.3. Sediment storage model for FIB

To determine the amount of FIB stored in the sediment bed, the mass balance equation was applied:

$$\rho_s A_s H_s \frac{dC_s}{dt} = v_s A_s f \frac{\rho_s}{TSS} C - v_b A_s \rho_s C_s - k_b A_s H_s \rho_s C_s \quad (9)$$

where  $\rho_s$  is the sediment wet bulk density [kg/m<sup>3</sup>],  $A_s$  is the sediment surface area of the study area [m<sup>2</sup>],  $H_s$  is the mixing depth of the sediment [m],  $f$  is the fraction of particle-associated FIB [–],  $TSS$  is the total suspended solids concentration in the water column [kg/m<sup>3</sup>],  $v_b$  is the sediment burial velocity [m/s], and  $k_b$  is the FIB die-off rate in sediment [1/s] [12,34–36].

2.3. Numerical methods

An analysis is required in order to obtain accurate solutions from a continuous partial differential equation (PDE), using an appropriate discrete approximation. In this study, the FIB transport model was solved via different numerical methods. Four different schemes were used, including upstream, forward time centered space (FTCS), Dufort-Frankel, and Crank-Nicolson methods (see Fig. 2); specific information for the four numerical schemes is described in Table 1 [28,29].

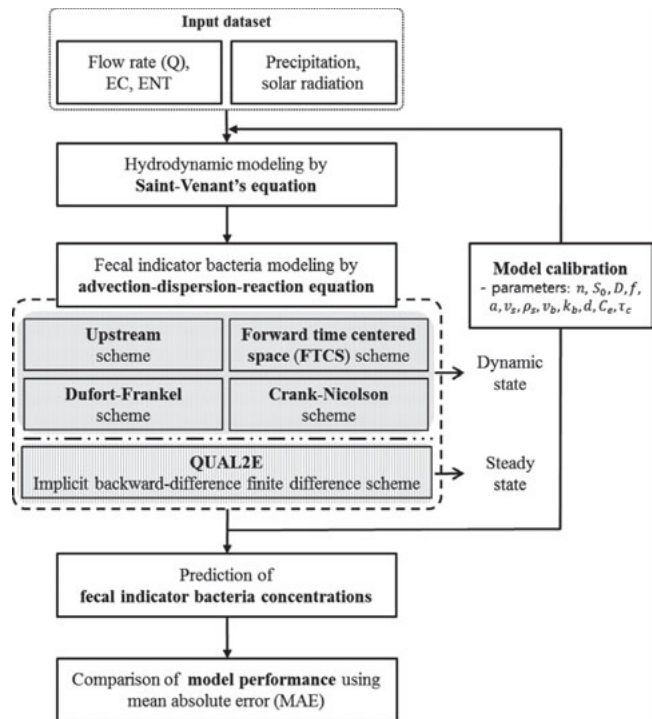


Fig. 2. Schematic of FIB modeling using four dynamic models and one steady state model.

Table 1  
Four numerical methods with details of approximation method and formula

Method	Scheme	Formula
Upstream method	$\frac{C_j^{i+1} - C_j^i}{\Delta t} = D \frac{C_{j+1}^i - 2C_j^i + C_{j-1}^i}{(\Delta z)^2} - u \frac{C_j^i + C_{j-1}^i}{\Delta z} - kC_j^i$	$C_j^{i+1} = (s + \frac{c}{2})C_j^i + (1 - k\Delta t - 2s)C_j^i + (s - \frac{c}{2})C_{j+1}^i$
FTCS method	$\frac{C_j^{i+1} - C_j^i}{\Delta t} = D \frac{C_{j+1}^i - 2C_j^i + C_{j-1}^i}{(\Delta z)^2} - u \frac{C_j^i + C_{j-1}^i}{\Delta z} - kC_{j+1}^i$	$C_j^{i+1} = (s + c)C_{j-1}^i + (1 - 2s - c - k\Delta t)C_j^i + sC_{j+1}^i$
Dufort Frankel method	$\frac{C_j^{i+1} - C_j^{i-1}}{2\Delta t} = D \frac{C_{j+1}^i - (C_j^{i+1} + C_j^{i-1}) + C_{j-1}^i}{(\Delta z)^2} - u \frac{C_j^{i+1} + C_j^{i-1}}{2\Delta z} - k \frac{C_j^{i+1} + C_j^{i-1}}{2}$	$C_j^{i+1} = \frac{c + 2s}{1 + 2s + k\Delta t} C_{j-1}^i - \frac{c - 2s}{1 + 2s + k\Delta t} C_{j+1}^i + \frac{1 - 2s - k\Delta t}{1 + 2s + k\Delta t} C_j^{i-1}$
Crank Nicolson method	$\frac{\partial C}{\partial t} \Big _j^{i+\frac{1}{2}} = \frac{1}{2} \left[ \frac{C_{j+1}^i - C_{j-1}^i}{2\Delta t} + \frac{C_{j+1}^{i+1} - C_{j-1}^{i+1}}{2\Delta t} \right]$	$-(c + 2s)C_{j-1}^{i+1} + (4 + 4s + 2k\Delta t)C_j^{i+1} - (2s - c)C_{j+1}^{i+1} = (c + 2s)C_{j-1}^i + (4 - 4s + 2k\Delta t)C_j^i - (2s - c)C_{j+1}^i$

$t$  is time [s],  $x$  is distance [m],  $C$  is the FCB concentration [MPN/100 ml],  $u$  is the depth average flow velocity [m/s],  $D$  is the dispersion coefficient [m<sup>2</sup>/s],  $k$  is the first-order decay coefficient [1/s], and  $s$  is  $D \frac{\Delta t}{(\Delta z)^2}$ ,  $c$  is  $u \frac{\Delta t}{\Delta z}$ . The different numerical methods according to  $i$  and  $j$  are used to approximate the solution at a finite set of  $x$  and  $t$ .

The FTCS method uses a forward-difference form for approximating the time and central-difference for the spatial derivative. This scheme is relatively efficient to implement because the values of  $C_j^{i+1}$  can be updated independently of each other. Thus, this scheme could be a better solution for a hyperbolic differential equation than using a parabolic differential equation. In the upstream method, the backward-difference form uses  $u \frac{\partial C}{\partial z}$  for the spatial derivative, the forward-difference form for the time derivative, and the centered-difference form for the space derivative. Another numerical method is the Dufort-Frankel method, which uses the approximation  $C_j^i \cong \frac{1}{2} (C_j^{i+1} + C_j^{i-1})$  for the reaction term. The Crank-Nicolson method is used when time-accurate solutions are important.

#### 2.4. QUAL2E model

The QUAL2E model, primarily developed by the U.S. Environmental Protection Agency (EPA), is an enhanced steady state model that is used to predict the water quality of a riverine system. This model can simulate up to 15 user-defined water quality parameters determined in well-mixed stream. It assumes that transport mechanisms (e.g., advection and dispersion) are significant only in a longitudinal direction. This model can simulate

up to 15 water quality parameters and consider multiple polluting discharges, withdrawals, tributary flows, and incremental inflows [30]:

$$\frac{\partial M}{\partial t} = \frac{\partial \left( A_x D_L \frac{\partial C}{\partial x} \right)}{\partial x} dx - \frac{\partial (A_x \bar{U} C)}{\partial x} dx + (A_x dx) \frac{dC}{dt} + s \quad (10)$$

where  $M$  is the mass [kg],  $A_x$  is the cross-sectional area [m<sup>2</sup>],  $D_L$  is the longitudinal dispersion coefficient [m<sup>2</sup>/s],  $\bar{U}$  is the mean river velocity [m/s],  $C$  is the constituent concentration [kg/s],  $x$  is the distance [m],  $t$  is the time [s], and  $s$  is the external source or sink [kg/s]. A complete description of the model is available in the QUAL2E model documentation [30]. As a steady state model, it has a limited ability to handle temporal variability in the riverine system. Here, in order to evaluate the potential for predicting FIB, the performance model compared this model with other dynamic models through their mean absolute errors (MAEs).

### 3. Results and discussion

The hydrodynamic module for water balance was calibrated and validated by comparing the observed and predicted water surface elevations at S4 (Fig. 1).

The determined values associated with the water quantity parameters were then used for further FIB predictions [11,37]. In each figure, S12, S23, and S34 denote the section between each monitoring site (e.g., between S1 and S2, S2 and S3, and S3 and S4, respectively).

### 3.1. QUAL2E simulation

To simulate FIB concentration under steady-state conditions, QUAL2E is applied using a one-dimensional advection-dispersion mass transport equation. In this case, based on a number of computational elements the GJC is modeled as a series of completely mixed reactors. Sub reaches have the same geometric properties, including riverbed slope, channel cross section, and Manning's roughness; they also have the same hydrodynamic (e.g., dispersion) and biological (e.g., decay rate) properties.

For computational segregation, the 12 km long GJC was divided into three sub-reaches (of unequal length), with each sub-element length being 500 m. The geometric properties of the sub reaches used were the same as the dynamic model properties. The flow rate and fecal coliform concentrations were calibrated during dry weather conditions. As a result of QUAL2E model application under all conditions, the EC and ENT concentrations displayed the worst agreement among the five methods, due to limitations of the kinetic module; the model only considers one parameter (coliform decay) depending on the water temperature [38,39].

### 3.2. Dry weather conditions

Figs. 3 and 4 show the spatiotemporally predicted and observed EC and ENT concentrations in GJC under dry weather conditions. In the figures, the horizontal axes represent the monitoring times in August 2007, and the vertical axes indicate the logarithmic FIB concentrations. The figure shows that the EC and ENT concentrations decreased during an increase of solar intensity (8:00–13:00); in contrast, the FIB concentrations increased during a decrease of solar intensity (13:00–18:00).

From Fig. 3, the EC concentration predicted by FTCS is in better agreement with the observed values than the other numerical methods, as the approximations in FTCS are more accurate [29]; the MAE values are 0.14 (FTCS), 0.19 (upstream), 0.22 (Dufort-Frankel), 0.24 (Crank-Nicolson), and 0.37 (QUAL2E), as shown Table 2. Similarly, the FTCS method shows the highest performance in predicting ENT during dry weather conditions; the MAE values are 0.37 (FTCS), 0.45 (upstream), 0.45 (Dufort-Frankel), 0.38 (Crank-Nicolson), and 0.38 (QUAL2E). The model accuracy of EC is relatively high when using the FTCS method, as compared to ENT. In previous studies, it has been shown that implicit

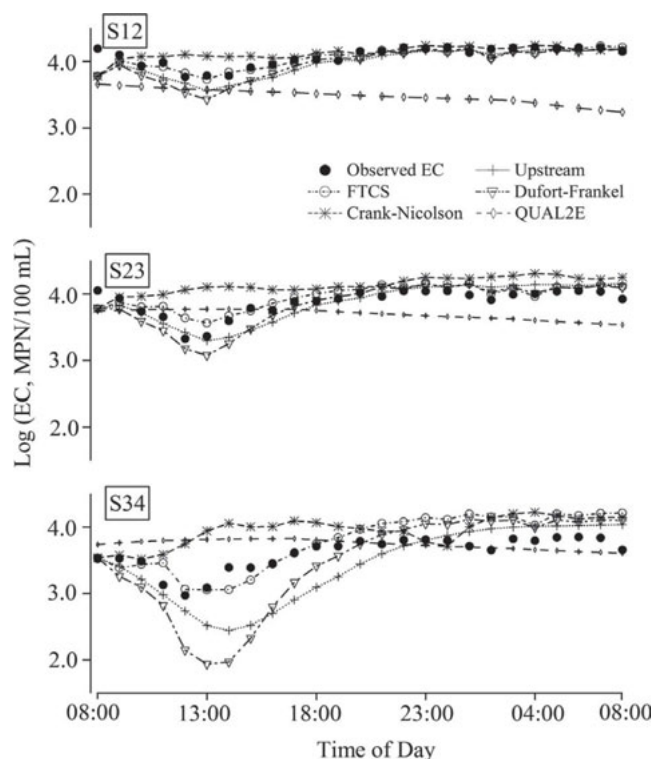


Fig. 3. Hourly variations of observed and predicted EC concentrations for different numerical schemes (upstream, FTCS, Dufort-Frankel, Crank-Nicolson, and QUAL2E) at averaged monitoring sections (S12, S23, S34) under dry weather conditions. Observed and predicted FIB concentrations were log-transformed. The horizontal axes indicate the monitoring period in 2007.

numerical schemes are more accurate than explicit schemes because of their numerical stability [40]. In a comparison of prediction accuracy under dry weather conditions, however, the explicit methods displayed better performance than implicit methods. It is posited here that this difference may have resulted from a reduction of the time increment, thereby causing divergence and a local instability that produced a critical force equilibrium in the implicit method [41,42].

### 3.3. Wet weather conditions

Figs. 5 and 6 present the spatiotemporally predicted and observed EC and ENT concentrations in the GJC under wet weather condition. It can be seen that the FIB concentrations did not follow the transport pattern from the dry weather conditions. However, the FIB concentrations increased when the rainfall intensity increased.

For EC and ENT simulations for wet weather conditions, two numerical models were selected, in the order of accuracy based on dry weather results. Unlike dry weather conditions, however, both of the predicted FIB concentrations obtained by the upstream method were

Table 2  
Mean absolute error (MAE<sup>a</sup>) between simulated and observed data

FIB concentration Log (MPN/100 ml)	Site	Dry weather conditions														
		Upstream			FTCS			Dufort-Frankel			Crank-Nicolson			QUAL2E		
		Min	Max	MAE	Min	Max	MAE	Min	Max	MAE	Min	Max	MAE	Min	Max	MAE
EC	Total sites	2.44	4.19	0.19	3.05	4.23	0.14	1.94	4.19	0.22	3.52	4.31	0.24	3.24	3.83	0.37
	S12	3.56	4.19	0.11	3.73	4.23	0.07	3.43	4.19	0.12	3.78	4.24	0.10	3.24	3.66	0.60
	S23	3.29	4.15	0.12	3.56	4.16	0.11	3.07	4.16	0.13	3.78	4.31	0.28	3.53	3.77	0.28
	S34	2.44	4.04	0.33	3.05	4.21	0.24	1.94	4.11	0.41	3.52	4.22	0.35	3.61	3.83	0.24
ENT	Total sites	1.29	3.40	0.45	1.68	3.47	0.37	0.83	3.42	0.45	2.13	3.48	0.38	2.77	3.32	0.28
	S12	2.11	3.40	0.36	2.17	3.47	0.34	2.11	3.42	0.37	2.28	3.48	0.35	2.77	3.24	0.24
	S23	1.86	3.24	0.50	2.00	3.24	0.48	1.82	3.19	0.53	2.13	3.32	0.34	3.01	3.30	0.21
	S34	1.29	3.13	0.48	1.68	3.31	0.28	0.83	3.25	0.47	2.29	3.27	0.47	3.06	3.32	0.41

FIB concentration Log (MPN/100 ml)	Site	Wet weather conditions					
		Upstream			FTCS		
		Min	Max	MAE	Min	Max	MAE
EC	Total sites	3.07	4.56	0.22	3.88	5.01	0.78
	S12	3.07	4.55	0.22	4.51	5.01	0.89
	S23	3.74	4.43	0.22	4.00	4.80	0.81
	S34	3.81	4.56	0.24	3.88	4.87	0.64
ENT	Total sites	2.86	4.45	0.31	2.90	4.86	0.73
	S12	2.86	4.44	0.35	4.24	4.86	0.99
	S23	3.32	4.36	0.28	3.79	4.71	0.58
	S34	2.90	4.45	0.30	2.90	4.79	0.62

<sup>a</sup>MAE =  $\left[ n^{-1} \sum_{i=1}^n |Y_{obs} - Y_{pre}| \right]$ , where  $Y_{obs}$  and  $Y_{pre}$  are observed values and predicted values, respectively, and n is the number of points.

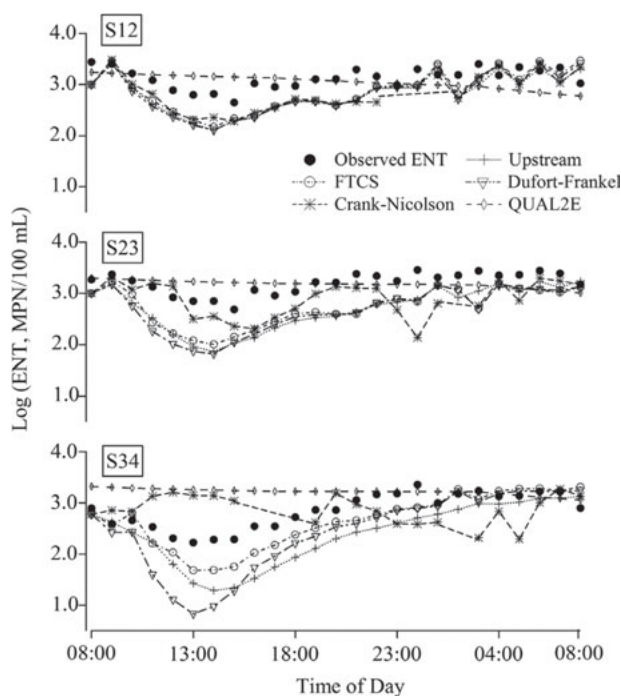


Fig. 4. Hourly variations of observed and predicted ENT concentrations for different numerical schemes at averaged monitoring sections under dry weather conditions. Observed and predicted ENT concentrations were log-transformed.

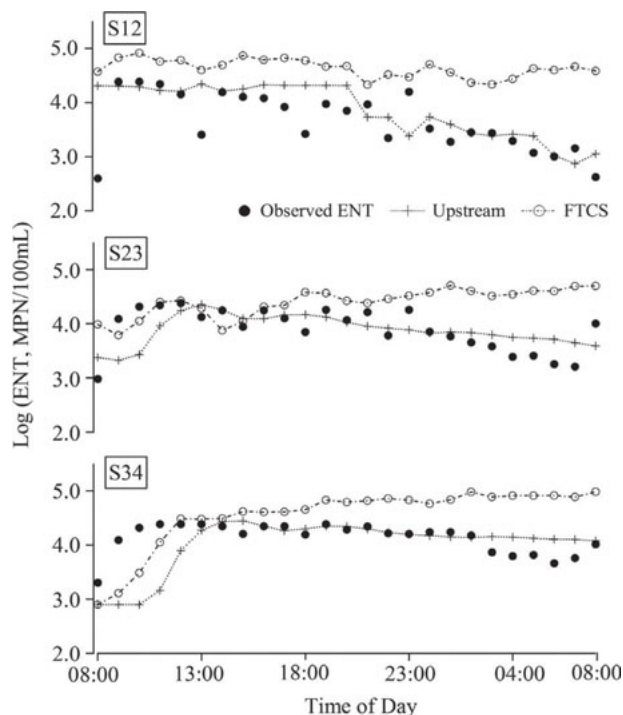


Fig. 6. Hourly variations of observed and predicted ENT concentrations for different numerical schemes at averaged monitoring sections under wet weather conditions. Observed and predicted ENT concentrations were log-transformed.

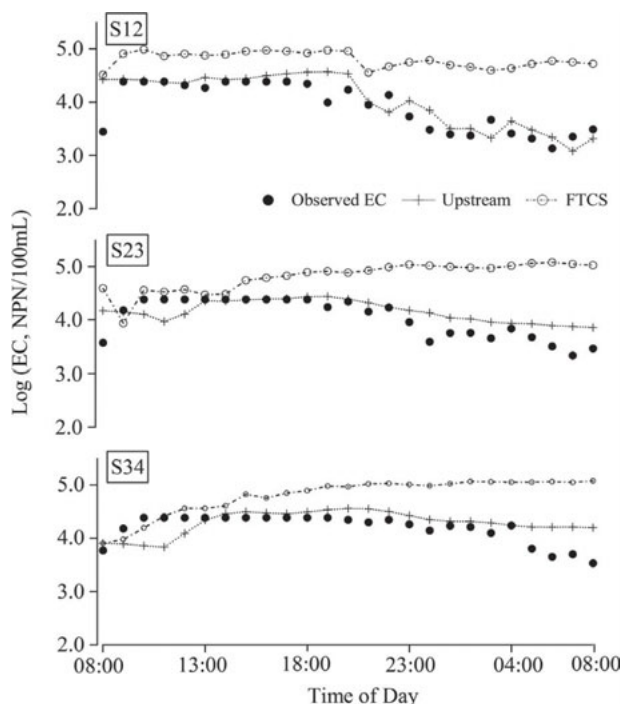


Fig. 5. Hourly variations of observed and predicted EC concentrations for different numerical schemes at averaged monitoring sections under wet weather conditions. Observed and predicted EC concentrations were log-transformed.

in better agreement with the observed values than for the FTCS method; the MAE values were 0.22 (upstream) and 0.78 (FTCS) for EC, and 0.31 (upstream) and 0.73 (FTCS) for ENT.

#### 4. Conclusions

In this study, a comprehensive spatiotemporal monitoring of two FIB was conducted in the GJC, a highly urbanized area in Korea. Based on the monitoring data, five models were investigated in an attempt to determine an appropriate prediction model for FIB concentrations based on a comparison of model accuracies; these models included four different dynamic models (FTCS, upstream, Dufort-Frankel, and Crank-Nicolson methods), and one steady state model (QUAL2E). From the FIB concentrations during dry weather conditions, the FTCS model displayed the highest prediction accuracy among the five models. The upstream model, however, revealed the best performance under wet weather conditions. This result implies that the upstream scheme can be utilized to predict FIB concentrations released from nonpoint sources during wet weather conditions. The comparison of model performance between dynamic models and steady state also indicates that the

widely used QUAL2E model cannot be implemented as an FIB prediction tool under 'best management' practices. Consequently, a summary of these modeling results suggests that an appropriate model can ensure an accurate prediction of FIB concentrations in a riverine system; this model also needs to consider complex conditions. From this study, we expect that the modeling approaches presented here can provide an alternative insight into FIB modeling from an objective assessment point-of-view, and that these models will be used as the basis for implementing a water quality forecasting system as a real-time management strategy in the near future in Korea.

### Acknowledgements

This research was supported by the Korea Ministry of Environment as "The Eco-innovation Project: Non-point source pollution control research group".

### References

- [1] A.P. Dufour and R.K. Ballentine, U.S. E.P.A. Regulations, S. Criteria, S. Division, Ambient water quality criteria for bacteria-1986, The Division, (1986).
- [2] S.M. Cha, S.W. Lee, Y.E. Park, K.H. Cho, S. Lee and J.H. Kim, Spatial and temporal variability of fecal indicator bacteria in an urban stream under different meteorological regimes, *Water Sci. Technol.*, 61 (2010) 3102.
- [3] S.M. Cha, Y.S. Ham, S.J. Ki, S.W. Lee, K.H. Cho, Y. Park and J.H. Kim, Evaluation of pollutants removal efficiency to achieve successful urban river restoration, *Water Sci. Technol.*, 59(11) (2009) 2101–2109.
- [4] G.A. Olyphant and R.L. Whitman, Elements of a predictive model for determining beach closures on a real time basis: the case of 63rd Street Beach Chicago, *Environ.monit.Assess.*, 98 (2004) 175–190.
- [5] J.J. Gannon and M.K. Busse, E. coli and enterococci levels in urban stormwater, river water and chlorinated treatment plant effluent, *Water Res.*, 23 (1989) 1167–1176.
- [6] G. Kim, J. Yur and J. Kim, Diffuse pollution loading from urban stormwater runoff in Daejeon city, Korea, *J. Environ.Manage.*, 85 (2007) 9–16.
- [7] J. Marsalek and Q. Rochfort, Urban wet-weather flows: sources of fecal contamination impacting on recreational waters and threatening drinking-water sources, *J. Toxicol. Env. Health., Part A*, 67 (2004) 1765–1777.
- [8] N. Tani, Y. Dohi, N. Kurumatani and K. Yonemasu, Seasonal distribution of adenoviruses, enteroviruses and reoviruses in urban river water, *Microbiol. Immunol.*, 39 (1995) 577.
- [9] L.W. Sinton, R.K. Finlay and P.A. Lynch, Sunlight inactivation of fecal bacteriophages and bacteria in sewage-polluted seawater, *Appl. Environ. Microb.*, 65 (1999) 3605.
- [10] J.D. Brookes, J. Antenucci, M. Hipsey, M.D. Burch, N.J. Ashbolt and C. Ferguson, Fate and transport of pathogens in lakes and reservoirs, *Environ. Int.*, 30 (2004) 741–759.
- [11] L. Sinton, C. Hall and R. Braithwaite, Sunlight inactivation of *Campylobacter jejuni* and *Salmonella enterica*, compared with *Escherichia coli*, in seawater and river water, *J. Water Health.*, 5 (2007) 357–365.
- [12] K.H. Cho, S.M. Cha, J.H. Kang, S.W. Lee, Y. Park, J.W. Kim and J.H. Kim, Meteorological effects on the levels of fecal indicator bacteria in an urban stream: A modeling approach, *Water Res.*, 44 (2010) 2189–2202.
- [13] G. Blom and H. Winkels, Modelling sediment accumulation and dispersion of contaminants in Lake IJsselmeer (The Netherlands), *Water Sci. Technol.*, 37 (1998) 17–24.
- [14] P.H. Struck, Relationship between sediment and fecal coliform levels in a Puget Sound Estuary, *J. Environ. Health JEVHAH* 50, (1988).
- [15] A. Eleria and R.M. Vogel, Predicting Fecal Coliform Bacteria Levels in the Charles River, Massachusetts, Usa1, *JAWRA J. Am. Water Resour. As.*, 41 (2005) 1195–1209.
- [16] G. Yagow, T. Dillaha, S. Mostaghimi, K. Brannan, C. Heatwole and M. L. Wolfe, TMDL modeling of fecal coliform bacteria with HSPF, The Society for engineering in agricultural, food and biological systems, (2001).
- [17] J.P. Connolly, A.F. Blumberg and J.D. Quadrini, Modeling fate of pathogenic organisms in coastal waters of Oahu, Hawaii, *J. Environ. Eng.*, 125 (1999) 398–406.
- [18] J.A. McCorquodale, I. Georgiou, S. Carnelos and A.J. Englande, Modeling coliforms in storm water plumes, *J. Environ. Eng. Sci.*, (2004) 419–431.
- [19] L. Liu, M.S. Phanikumar, S.L. Molloy, R.L. Whitman, D.A. Shively, M.B. Nevers, D.J. Schwab and J.B. Rose, Modeling the transport and inactivation of E. coli and enterococci in the near-shore region of Lake Michigan, *Environ. Sci. Technol.*, 40 (2006) 5022–5028.
- [20] E.A. Matson and S.G. Horner, Pollution indicators and other microorganisms in river sediment, *J. Water Poll. Control Fed.*, 50(1) (1978) 13–19.
- [21] G. Yagow and V. Shanholtz, TARGETING SOURCES OF FECAL COLIFORM IN MOUNTAIN RUN, ASAE Paper No. 98–2031 (1998).
- [22] C.G. Uchrin and W.J. Weber, Modeling suspended solids and bacteria in Ford Lake, *J. Environ. Eng. Division*, 107(5) (1981) 975–993.
- [23] R.J. Wilkinson, A. Jenkins, M. Wyer and D. Kay, Modelling faecal coliform dynamics in streams and rivers, *Water Res.*, 29(3) (1995) 847–855.
- [24] B.M. Streets and P.A. Holden, A mechanistic model of runoff-associated fecal coliform fate and transport through a coastal lagoon, *Water Res.*, 37(3) 589–608.
- [25] A.I. Stamou, Improving the numerical modeling of river water quality by using high order difference schemes, *Water Res.*, 26(12) (1992) 1563–1570.
- [26] X. Wang, Z. Meng, B. Chen, Z. Yang and C. Li, Simulation of nitrogen contaminant transportation by a compact difference scheme in the downstream Yellow River, China, *Communications in Nonlinear Sci. Numer. Simul.*, 14 (2009) 935–945.
- [27] G. Gao, R.A. Falconer and B. Lin, Numerical modelling of sediment-bacteria interaction processes in surface waters, *Water Res.*, (2011).
- [28] S. Najafi and H. Hajinezhad, Solving One-dimensional Advection-Dispersion with Reaction Using Some Finite-Difference Methods, *Appl. Math. Sci.*, 2 (2008) 2611–2618.
- [29] Y. Yang, L. Wilson, M. Makela and M. Marchetti, Accuracy of numerical methods for solving the advection-diffusion equation as applied to spore and insect dispersal, *Ecol. Modell.*, 109 (1998) 1–24.
- [30] L.C. Brown and T.O. Barnwell, The enhanced stream water quality models QUAL2E and QUAL2E-UNCAS: Documentation and User Manual. EPA/600/3-87/007, Environ. Res. Laboratory, EPA, Athens, GA, (1987).
- [31] S.J. Ki, Y.G. Lee, S.W. Kim, Y.J. Lee and J.H. Kim, Spatial and temporal pollutant budget analyses toward the total maximum daily loads management for the Yeongsan watershed in Korea, *Water Sci. Technol.*, 55(1–2) 367–374.
- [32] S.M. Cha, S.J. Ki, K.H. Cho, H. Choi and J.H. Kim, Effect of environmental flow management on river water quality: a case study at Yeongsan River, Korea, *Water Sci. Technol.*, 59(12) (2009) 2437–2446.

- [33] M.E. Keskin and N. Ağırlioğlu, A simplified dynamic model for flood routing in rectangular channels, *J. Hydrol.*, 202 (1997) 302–314.
- [34] G. Blom and H. Winkels, Modelling sediment accumulation and dispersion of contaminants in Lake IJsselmeer (The Netherlands), *Water Sci. Technol.*, 37 (1998) 17–24.
- [35] R.C. Jamieson, D.M. Joy, H. Lee, R. Kostaschuk and R.J. Gordon, Resuspension of sediment-associated *Escherichia coli* in a natural stream, *J. Environ. Qual.*, 34 (2005) 581–589.
- [36] S. Bai and W.S. Lung, Modeling sediment impact on the transport of fecal bacteria, *Water Res.*, 39 (2005) 5232–5240.
- [37] K.H. Cho, S.W. Lee, Y.S. Ham, J.H. Hwang, S.M. Cha, Y. Park and J.H. Kim, A new methodology for determining dispersion coefficient using ordinary and partial differential transport equations, *Water Sci. Technol.*, 59(11) (2009) 2197–2203.
- [38] F. Cubillo, B. Rodriguez and T. Barnwell Jr, A system for control of river water quality for the community of Madrid using QUAL2E. *Water Sci. Technol.*, 26 (1992) 1867–1873.
- [39] G. Brajesh, K. Murthy and L. Wei, Determination of fecal coliform loading and its impact on river water quality for TMDL development, *WEFTEC 2006*, 24 (2006) 3851–3874.
- [40] M. Dehghan, Numerical schemes for one-dimensional parabolic equations with nonstandard initial condition, *Appl. Math. Comput.*, 147 (2004) 321–331.
- [41] J. Sun, H. Lee and H. Lee, Comparison of implicit and explicit finite element methods for dynamic problems, *J. Mater. Process. Tech.*, 105 (2000) 110–118.
- [42] N. Rebelo, J.C. Nagtegaal and L.M. Taylor, Comparison of implicit and explicit finite element methods in the simulation of metal forming processes, in: Chenot, Wood, Zienkiewicz (Eds.), *Numer. Meth. Ind. Forming Processes*, (1992) 99–108.